

Pore-Pressure Generation and Liquefaction of Granular Soil Tested in Triaxial Conditions

Jacek Mierczyński, Andrzej Sawicki

Institute of Hydro-Engineering PAS, ul. Kościarska 7, 80-328 Gdańsk-Oliwa, Poland,
e-mails: mier@ibwpan.gda.pl, as@ibwpan.gda.pl

(Received June 22, 2009)

Abstract

The paper deals with modelling of pore-pressure generation in saturated sand subjected to triaxial cyclic loading in undrained conditions. The model proposed links the pore-pressure generation with the cyclic loading induced compaction of the same sand, but tested in fully drained conditions. The governing equation for the pore-pressure changes is derived from the assumption that no volumetric strain develops in saturated sand in undrained conditions. The numerical solutions are compared with experimental data, for a large number of loading cycles.

Key words: cyclic loadings, granular soils, triaxial conditions, pore-pressure generation, liquefaction.

1. Introduction

The paper discusses modelling the phenomena that take place during the cyclic loading of saturated sands, tested in undrained conditions, such as pore-pressure generation and liquefaction. These phenomena are of importance in earthquake geotechnics and in many other problems where cyclic loadings take place. The literature on this subject is quite extensive, see the book of Ishihara (1996) or the state-of-the-art paper by Sawicki and Mierczyński (2006).

Most of the previous research dealt with the behaviour of granular soils subjected to cyclic loading in simple shear tests. There was available experimental data dealing with tests performed in other devices like, for example, the triaxial cyclic apparatus which has been developed for these purposes quite recently. Such modern devices enable realization of even thousands of loading cycles. Sawicki et al (2009) study the behaviour of dry sand “Skarpa” tested in the cyclic triaxial apparatus *Enel-Hydro*. They have determined the deformations of sand caused by cyclic loads, particularly the compaction curves, and proposed a constitutive equation describing this phenomenon.

In the present paper, the above mentioned results will be applied to simulate the undrained behaviour of sand subjected to cyclic loadings, like the phenomena of pore-pressure generation and liquefaction. Theoretical predictions will be compared with experimental results.

2. Compaction of Dry Sand in Triaxial Conditions

Sawicki et al (2009) have derived the following incremental constitutive equation describing the permanent volumetric changes (compaction) of sand due to cyclic loadings:

$$d\varepsilon_v^c = \left[\frac{d\varepsilon_v^*}{dN} \beta \ln(1 + \alpha N) + \frac{\alpha \beta \varepsilon_v^*}{1 + \alpha N} \right] dN, \quad (1)$$

where:

- α, β – constants,
- N – number of loading cycles, treated as a continuous variable,
- ε_v^c – volumetric strain due to cyclic loading,
- ε_v^* – permanent volumetric strain after $N = 10^4$ cycles.

The permanent strain ε_v^* depends on the deviatoric cyclic stress amplitude Δq , deviatoric stress $q = \sigma'_1 - \sigma'_3$ and mean effective stress $p' = (\sigma'_1 + 2\sigma'_3)/3$, where: σ'_1 and σ'_3 – vertical and horizontal effective stresses, respectively.

Eq. (1) is valid for a large number of loading cycles ($N = O(10^4)$). Its distinguishing feature is that it takes into account the initial stress state around which the cyclic loading takes place, defined by the deviatoric strain q and the mean effective stress p' .

3. Modelling the Pore-Pressure Generation and Liquefaction

In order to simulate the undrained behaviour of saturated sand subjected to cyclic loading, we have to determine the incremental equation describing the accumulation of excess pore-pressure. This important relation will be determined from Eq. (1), assuming

$$d\varepsilon_v = d\varepsilon_v^c + d\varepsilon_v^s = 0, \quad (2)$$

where: $d\varepsilon_v^s$ – volumetric strain due to change of the mean effective stress.

The condition (2) defines the undrained behaviour of saturated sand, as it is commonly accepted. In this case no volumetric changes take place, because pore-water imposes constraints on these changes. Obviously, it is an approximation because some addition of gas into the pore-water significantly increases its compressibility, so the condition (2) can be violated. However, in the experiments reported in this paper, the pore-water had been de-aerated, so we can assume that Eq. (2) is valid.

Fig. 1 shows a typical experimental record showing the effective stress path during the undrained shearing of saturated sand in triaxial conditions. The cyclic

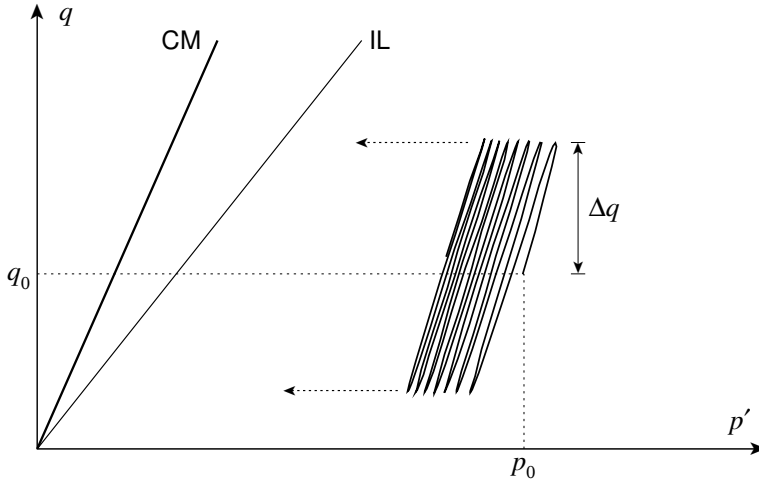


Fig. 1. Effective stress path during cyclic shearing of sand in undrained conditions

shearing, characterized by the constant shear stress amplitude Δq , starts at the point described by the mean effective stress $p' = p_0$ and the shear stress $q = q_0 = \text{const}$. During cyclic loading, the excess pore-pressure u is generated, so the mean effective stress decreases, according to the following relation:

$$p' = p_0 - u. \tag{3}$$

Subsequently, the effective stress path gradually moves to the left.

Eq. (1) can be written in the following form:

$$d\varepsilon_v^c = \left[\frac{d\varepsilon_v^*}{dN} F(N) + \varepsilon_v^* \frac{dF}{dN} \right] dN = \left[\frac{d\varepsilon_v^*}{dp'} \frac{dp'}{dN} F(N) + \varepsilon_v^* \frac{dF}{dN} \right] dN, \tag{4}$$

where: $F(N) = \beta \ln(1 + \alpha N)$.

The strain increment $d\varepsilon_v^s$ can be written as:

$$d\varepsilon_v^s = \frac{d\varepsilon_v^s}{dp'} dp'. \tag{5}$$

Using (3) one obtains:

$$dp' = -du. \tag{6}$$

Combining Eqs. (4), (5) and (6) with Eq. (2) leads to:

$$\frac{du}{dN} = \varepsilon_v^* \frac{dF}{dN} \left[F(N) \frac{d\varepsilon_v^*}{dp'} + \frac{d\varepsilon_v^s}{dp'} \right]^{-1}. \tag{7}$$

4. Numerical Examples against Experimental Data

4.1. Experimental Results

Fig. 2 shows the example of pore-pressure changes measured during the cyclic triaxial test. For a detailed description of testing procedure see Świdziński and Mierczyński (2005) and Sawicki et al (2009).

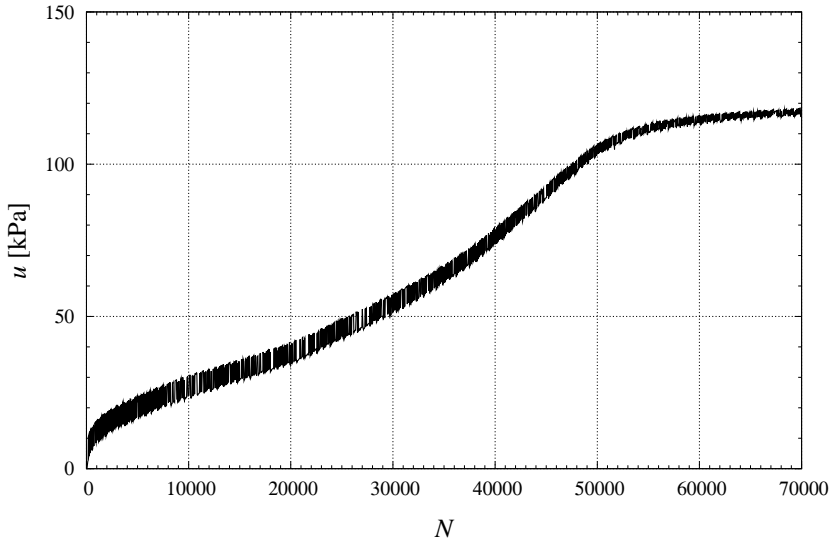


Fig. 2. Results of the cyclic undrained triaxial test for medium-dense “Skarpa” sand – pore-pressure changes vs. number of loading cycles

The sample made of saturated, medium dense “Skarpa” sand was first isotropically consolidated to the confining pressure $p' = 168$ kPa. In the next step, the deviatoric stress $q_0 = 96$ kPa was applied (in drained conditions). This initial stress state ($q_0 = 96$, $p' = 200$) corresponds to the condition:

$$\eta = \eta_0 = \frac{q_0}{p'_0} = \frac{\eta'}{2}, \quad (8)$$

where:

- $\eta = q/p'$ – non-dimensional stress ratio,
- η_0 – stress ratio corresponding to the initial stress state,
- $\eta' = 0.96$ – stress ratio corresponding to the instability line.

After applying the initial stress, the void ratio of the sand was $e = 0.53$, which together with the applied value of p_0 means a dilative initial state. After closing

pore water valves, the sample was subjected to cyclic loading with the amplitude $\Delta q = 25$ kPa and period $T = 1$ s:

$$\sigma_3 = \text{const}, \quad \sigma_1 = \sigma_3 + q_0 + \Delta q \sin\left(\frac{2\pi t}{T}\right), \quad (9)$$

where: σ_3 – total horizontal stress equal to the pressure in the triaxial cell.

Cyclic undrained loading causes an increase of pore-pressure as shown in Fig. 2. Initially, the shape of the curve $u(N)$ is similar to compaction curves $\varepsilon_v^c(N)$. The increase of pore-pressure causes gradual reduction of the mean effective stress. When the effective stress path approaches the instability line ($N > 30\,000$) the rate of pore-pressure generation slowly increases. However, further loading ($N > 45\,000$) leads to decrease of the pore-pressure generation rate and pore-pressure slowly reaches its final value of about 120 kPa.

This behaviour can be explained by the initial dilative state of the sample: the cyclic loading induced tendency for compaction is balanced by dilation as the effective stress path approaches the Coulomb-Mohr line.

4.2. Numerical Procedure

Eq. (7) has been solved numerically using an explicit, two-step Euler method (Potter 1977) with the initial conditions:

$$u(N = 0) = 0, \quad p'(N = 0) = p_0. \quad (10)$$

Writing Eq. (7) in the following form:

$$\frac{du}{dN} = G(p', N), \quad (11)$$

and introducing discrete equivalents of continuous functions N , p' and u , the following result is obtained:

$$U_{i+1} = U_i + G\left(P'_{i+1/2}, N_{i+1/2}\right) \cdot \delta_N, \quad (12)$$

where:

$$N_{i+1/2} = N_i + \frac{\delta_N}{2}, \quad (13)$$

$$P'_i = p_0 - U_i, \quad (14)$$

$$U_{i+1/2} = U_i + G\left(P'_i, N_i\right) \frac{\delta_N}{2}. \quad (15)$$

Recall that the function $F(N)$ in Eq. (7) is the following:

$$F(N) = \beta \ln(1 + \alpha N), \quad (16)$$

where: $\beta = 0.18$, and $F(N = 10^4) = 1$ gives $\alpha = 0.02577$.

It is assumed that the following relation, proposed by Wichtmann et al (2005), describes the dependence of accumulated strain ε_v^* on the mean effective stress p' (for constant q_0 and Δq):

$$\varepsilon_v^* = C_1 \exp \left[-C_p \left(\frac{p_0}{p_{\text{ref}}} - 1 \right) \right], \quad (17)$$

where the reference pressure $p_{\text{ref}} = 100$ kPa. The experimental data and the function (17) are shown in Fig. 3, for $C_1 = 1.5 \times 10^{-3}$ and $C_p = 1.52$.

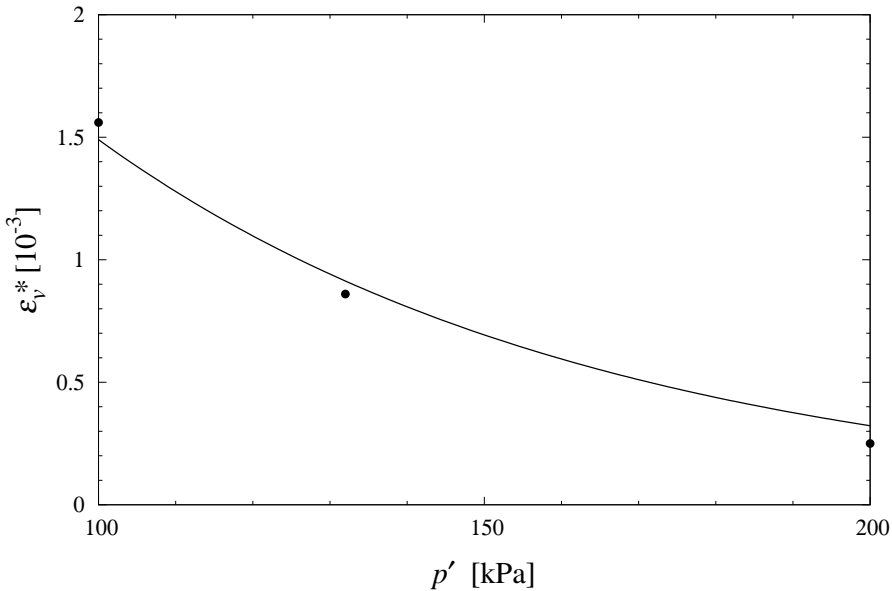


Fig. 3. Dependence of accumulated strain ε_v^* on the mean effective stress p' – experimental data vs. analytical approximation proposed by Wichtmann et al (2005)

The value of sand compressibility coefficient $\kappa^s = d\varepsilon_v^u/dp'$ was determined from the results of isotropic compression tests. The numerical results presented below were obtained for $\kappa^s = 1.63 \times 10^{-8} \text{ m}^2/\text{N}$.

4.3. Results of Calculations

The experimental data (from Fig. 2) are compared with the numerical results, see Fig. 4. Initially, the calculated values of pore-pressure are close to the values measured in the experiment. For $N \approx 27\,000$ the computed values of du/dN increase rapidly when the denominator in the right-hand term of Eq. (7) approaches zero (which leads to the end of calculations):

$$F(N) \frac{d\varepsilon_v^*}{dp'} = \frac{d\varepsilon_v^s}{dp'} = -\kappa^s. \tag{18}$$

Note that $d\varepsilon_v^*/dp' < 0$ and $F(N) \geq 0$.

In this example, the calculated results are typical for a liquefaction phenomenon.

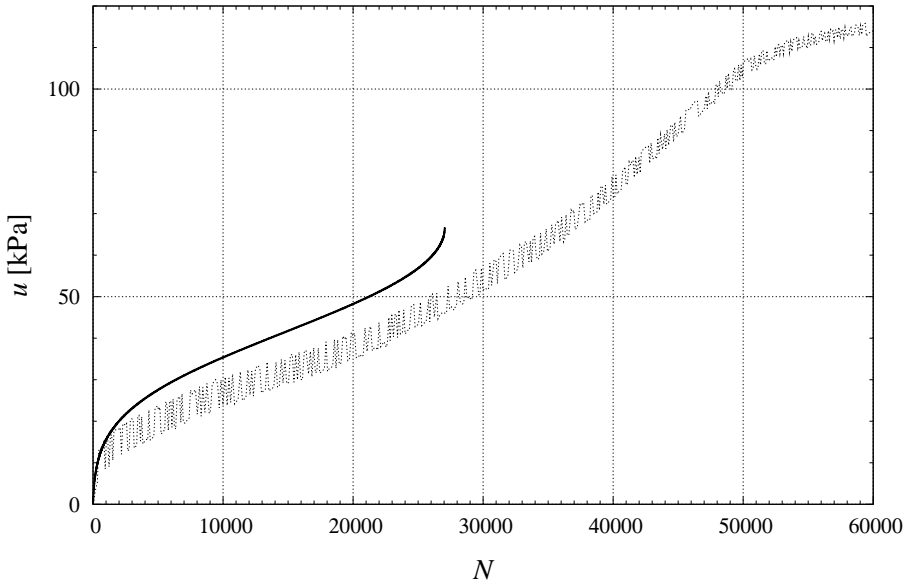


Fig. 4. Comparison of experimental data (dots) and numerical results (solid line)

The next example shows results of the calculations which take into account the effect of dilation.

It follows from the monotonic, pure shearing triaxial tests ($p' = \text{const}$), that the volumetric strain is a function of stress ratio η and can be approximated as:

$$\varepsilon_v^s(\eta) = -A \exp \left[B \left(\frac{\eta}{\eta''} \right) - 1 \right], \tag{19}$$

where: η'' corresponds to the Coulomb-Mohr failure condition. For a medium dense “Skarpa” sand $A \approx 4 \times 10^{-3}$, $B \approx 10$ and $\eta'' \approx 1.55$.

In this example the term $d\varepsilon_v^s/dp'$ in Eq. (7) is a function of both the mean effective stress p' and strain ratio η :

$$\frac{d\varepsilon_v^s}{dp'} = \left(\frac{\partial \varepsilon_v^s}{\partial p'} \right) + \left(\frac{\partial \varepsilon_v^s}{\partial \eta} \right) \frac{d\eta}{dp'}. \tag{20}$$

The results of calculations are shown in Fig. 5. Although there are some differences, the model proposed gives realistic predictions as it reflects the main features of the cyclic loading induced pore-pressure changes.

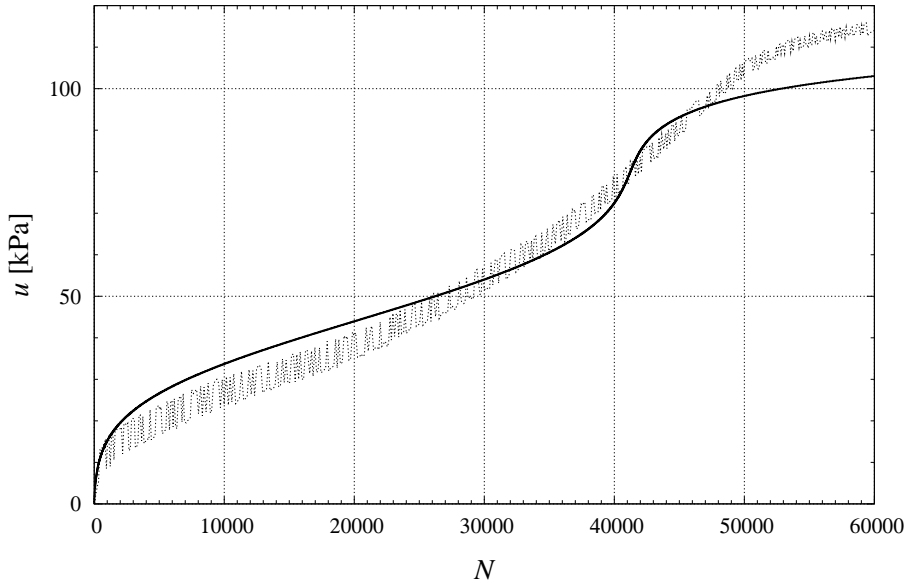


Fig. 5. Experimental data and numerical results with the effect of dilatancy included

The above results were obtained with a relatively simple assumption regarding the volumetric strain increment $d\varepsilon_v^s$. In further development of the model it is possible to introduce more advanced equations which enable determination of strain increments for a given stress path, see Sawicki (2007), Sawicki and Świdziński (2007).

5. Conclusions

The key results presented in this paper can be summarized as follows:

1. A simple theoretical model of cyclic loading induced pore-pressure generation is proposed. The model is based on the assumption that there exists a link between pore-pressure generation in undrained conditions and compaction in drained conditions.
2. The quality of the model proposed depends on proper determination of accumulated volumetric strains for a wide range of initial stress states.
3. Further research on this subject is necessary.

Acknowledgement

Research presented in this paper was supported by the Polish Ministry of Science and Higher Education: research grant No. 4 T07A 028 30.

References

- Ishihara K. (1996) *Soil Behaviour in Earthquake Geotechnics*, Clarendon Press, Oxford.
- Potter D. (1977) *Computational Physics*, PWN, Warsaw (in Polish).
- Sawicki A. (2007) A study on pre-failure deformations of granular soils, *Archives of Hydro-Engineering and Environmental Mechanics*, **54** (3), 183–206.
- Sawicki A., Mierczyński J. (2006) Development in modelling liquefaction of granular soils, caused by cyclic loads, *Applied Mechanics Reviews*, **59** (2), 91–106.
- Sawicki A., Mierczyński J., Świdziński W. (2009) Strains in sand due to cyclic loading in triaxial conditions, submitted to *Archives of Hydro-Engineering and Environmental Mechanics*, **56** (1–2), 63–98.
- Sawicki A., Świdziński W. (2007) Drained against undrained behaviour of granular soils, *Archives of Hydro-Engineering and Environmental Mechanics*, **54** (3), 207–222.
- Świdziński W., Mierczyński J. (2005) Instability line as a basic characteristic of non-cohesive soils, *Archives of Hydro-Engineering and Environmental Mechanics*, **52** (1), 59–85.
- Wichtmann T., Niemunis A., Triantafyllidis Th. (2005) Strain accumulation in sand due to cyclic loading: drained triaxial tests, *Soil Dynamics and Earthquake Engng.*, **25**, 967–979.